

PMT tests at UMD

Vlasios Vasileiou

Version 1.0

1st May 2006

Abstract

This memo describes the tests performed on three Milagro PMTs in UMD. Initially, pulse-height distributions of the PMT signals were made for different conditions. The dependence of the pulse heights with respect to the supply voltage, the photocathode illumination position and the PMT orientation was examined. Next, the dependence of the detection efficiency on the incidence angle and illumination position was examined. The main finding of this series of tests was that the PMT gain and detection efficiency depends strongly on the photocathode illumination position. Both parameters decrease as points far away from the top of the PMT and near the equator are illuminated.

Contents

1	Experimental setup	2
2	The tests	3
2.1	Pulse height spectra	3
2.1.1	Dark noise spectrum	3
2.1.2	Dependence on the supply voltage and PMT orientation.	3
2.1.3	Dependence on the illumination position	4
2.2	Detection efficiency	6
2.2.1	Dependence on the photocathode position	6
2.2.2	Dependence on the incidence angle	7
3	Discussion - Conclusion	9
4	Appendix	10
4.1	PMT Base and Signal pick-off circuit	10
4.2	Hamamatsu R5912 PMT Specifications	11
4.3	Absolute measurement of the detection efficiency of the PMT	15

1 Experimental setup

Three outrigger PMTs were tested (PMT details shown in Table 1). From these, just one of them PMT #1024 was extensively tested.

PMT#	S/N	Optimum HV (Volts)
1024	SA2979	1650
394	SA1073	1825
992	SA1483	1730

Table 1: Details of the PMTs tested

The PMTs are used in Milagro in a way that the signal and the supply voltage are carried in the same cable. A signal pick-off circuit is used to extract the signal from the cable that carries the supply voltage to the PMT. The circuits of the PMT base and signal pick-off circuit are shown in Appendix 4.1 on page 10.

For making the pulse height distributions, the PMT pulses were analysed by a Tektronix TDS2024 oscilloscope. The oscilloscope would measure their amplitude and send the results to a PC through the serial port. For the detection efficiency measurements a *Philips Scientific Model 706* discriminator and a 20ns dead-time scaler were used. The system was gated with a *LeCroy 222 Dual Gate Generator*. All the modules were mounted on a *LeCroy Model 1002A NIM Crate*.

The light source is composed of parts from Thorlabs and Nichia corp. Two black threaded tubes of 1' diameter and 2' and 3' length were the main body of the light source. Between the two tubes a neutral density filter with 1/100 (ND2) absorption factor was used. The light was produced by LEDs from the Nichia corporation. Their biggest advantage is that their spectral response is pretty narrow ($\sim 30\text{nm}$ FWHM) and that they are relatively stable under changes in temperature. At the ends of the tubes two end-caps were attached. The end-caps had a hole of $\sim 4.8\text{mm}$ diameter. One of the end-caps was used to firmly hold the LED and the other as a collimator. The resulting light beam had a very low opening angle of about 1deg .

The experimental tests required the light source to be positioned in predefined known locations and orientations with respect to the PMT face. A wooden structure was built for that reason. With the help of clamps the PMT and the light source could be mounted steadily on the structure. A photo of the structure with the light source and a broken PMT mounted on it, is shown in Figure 1.



Figure 1: PMT and light source support structure

2 The tests

2.1 Pulse height spectra

For all the tests except the dark noise spectrum, the light source was operated in pulsed mode. In the pulsed mode, a *BNC BL-2 Pulse Generator* was used for driving the light source and for triggering the oscilloscope. The light level was so low that the light source would emit at most two distinct photons after each pulse. The oscilloscope would digitize pulses occurring in a window, of width $\sim 100\text{ns}$, starting $\sim 110\text{ns}$ after the pulses. The dark rate of the PMT was about 2KHz , so on average there was just one dark noise hit digitized by the oscilloscope every $\sim 2 \cdot 10^5$ triggers. For the dark noise spectrum test, the light source was connected to a low voltage power supply and was operated in DC mode. The oscilloscope was then self triggering on the PMT pulses.

In all the following pulse height spectra, the pedestal is suppressed and the curves are normalised to have integral equal to 1.

2.1.1 Dark noise spectrum

The PMT (#1024) was in an optically shielded black box and the room lights were off. The PMT was in the vertical position (like in Milagro). The count rate was about $\sim 1.8\text{KHz}$. The oscilloscope had an internal limit on the minimum pulse amplitude it could be triggered by related to the volts/div scale of its display. For this measurement, the effective triggering threshold was at about 10mV . The supply voltage was 1800V .

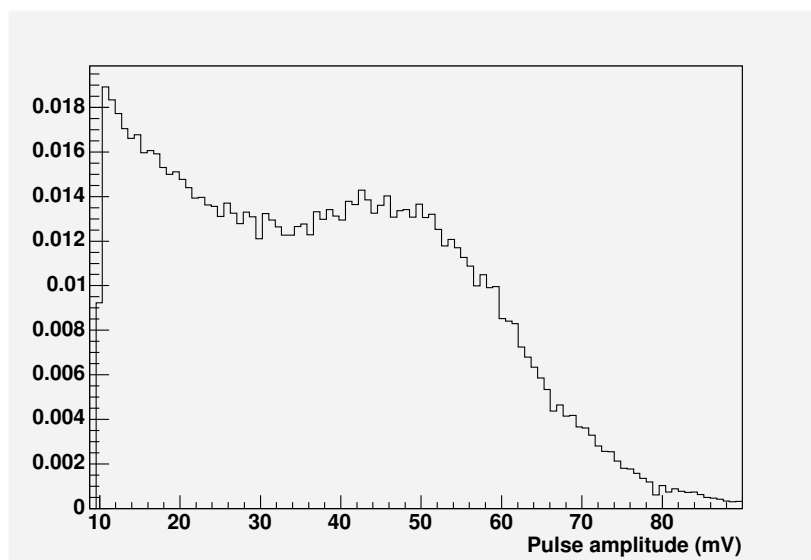


Figure 2: Dark noise pulse height distribution

2.1.2 Dependence on the supply voltage and PMT orientation.

PMT #1024 was tested. Pulse height distributions were made for different supply voltages (1600V , 1800V and 2000V), illumination positions (top and near the equator) and PMT orientations (horizontal and vertical). While in the horizontal orientation, a vector perpendicular to the top of the photocathode and pointing outwards, would point to the south.

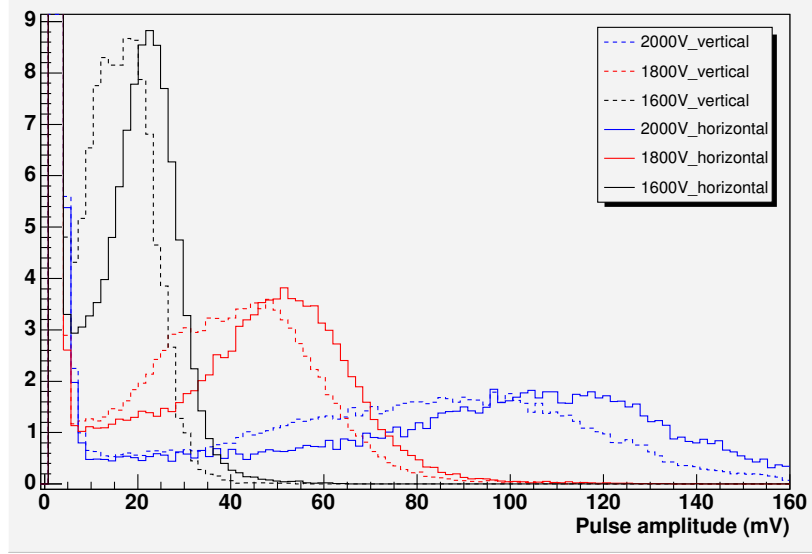
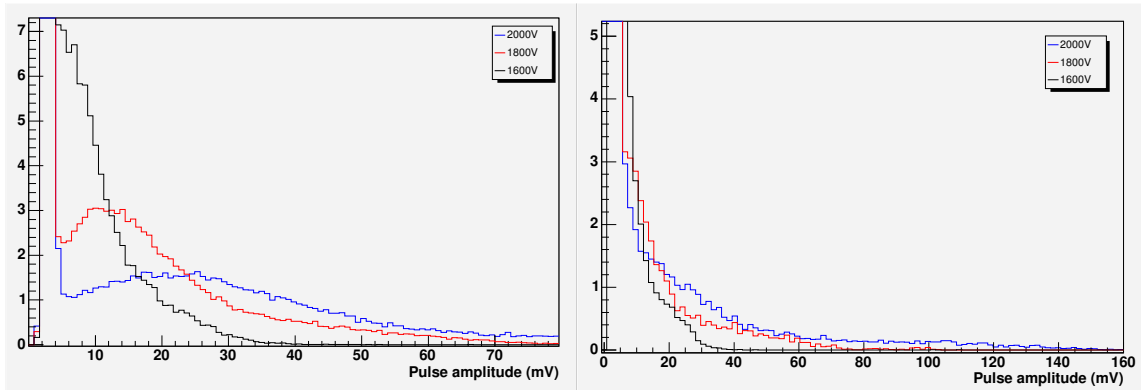


Figure 3: Pulse height distribution for illumination of the top of the photocathode



(a) PMT horizontal

(b) PMT vertical

Figure 4: Pulse height distribution for illumination of a point near the equator

2.1.3 Dependence on the illumination position

Pulse height distributions were made for different illumination positions on the photocathode. The supply voltage used was 1800V and the PMT orientation was vertical. Only one of the PMTs was extensively tested (PMT #1024). For the other two PMTs, only the side and top illumination positions were examined. Notice the sharp transition between 63° and 71° in table 2. It is worth noting that the width of the pulses stays almost the same independently on their height.

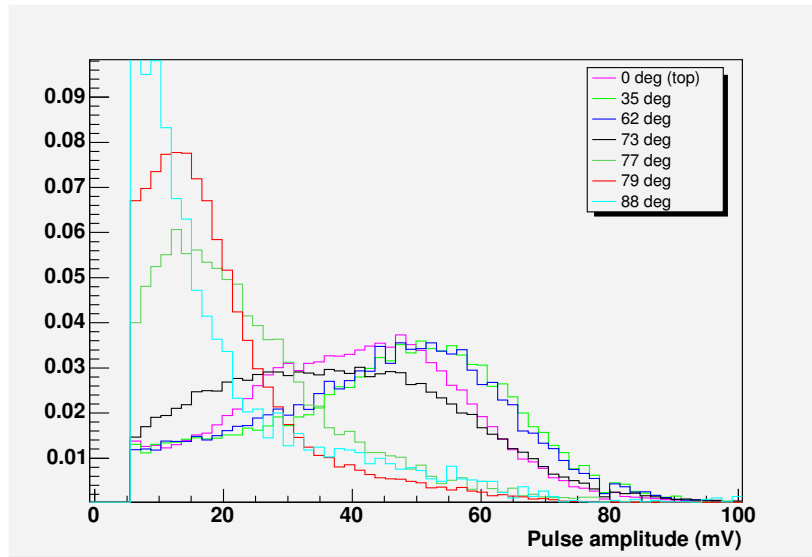


Figure 5: Pulse height distribution for illumination at different positions on the photocathode

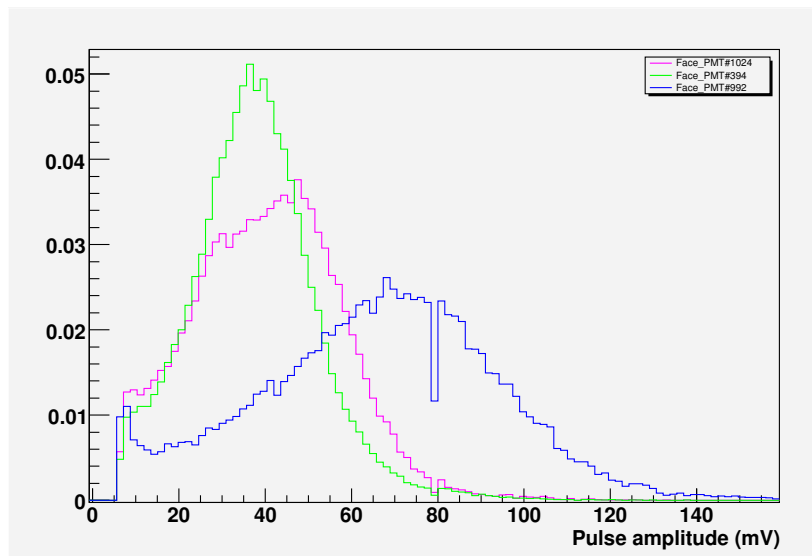


Figure 6: Pulse height distributions for illumination at the top of three different PMTs

Distance from top measured on the PMT surface (cm)	Distance from PMT axis (cm)	Angle (deg)	Most probable pulse height (mV)
0	0	0	46.98
3.9	3.85	29	52.64
7.0	6.7	52	51.85
8.6	7.9	63	40.55
9.6	8.4	71	18.88
10.1	8.6	75	11.68
12.2	9.6	90	4.6

Table 2: Most probable pulse height

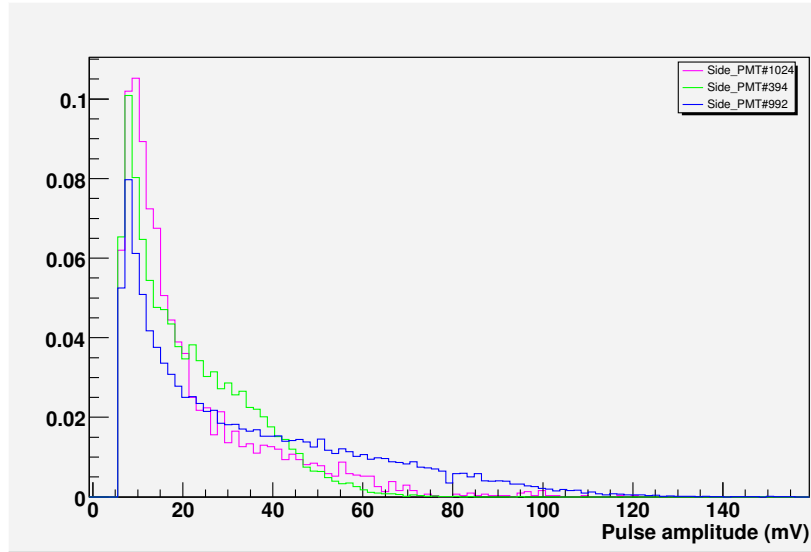


Figure 7: Pulse height distributions for illumination at the side of three different PMTs

2.2 Detection efficiency

2.2.1 Dependence on the photocathode position

The light source was operated at DC mode. There were seven different sets of measurements, each one corresponding to one of the illumination positions described above. Each set was composed of two background measurements followed by two signal measurements and then followed by two background measurements. The duration of each measurement was 10sec and in each, the number of pulses with amplitudes over 10mV¹ were counted. Only one of the PMTs was extensively tested (#1024). For the other two PMTs only the the ratio of side/top efficiency was measured.

Since the counting system couldn't measure the pulses over the pedestal (~ 5 mV) and under 10mV, the signal counts had to be multiplied by an appropriate factor. This factor, calculated from the pulse height distribution for each position, was equal to the ratio of the number of pulses with amplitudes higher than 5mV over the number of pulses with amplitudes higher than 10mV.

¹the lowest discrimination level of the discriminator

Angle of illumination position (deg)	Relative efficiency (%)		
	<i>PMT #1024</i>	<i>PMT #394</i>	<i>PMT #992</i>
0	100±0.52	100±0.49	100±0.84
29	92.38±0.48		
52	88.52±0.33		
63	62.74±0.32		
65	65.45±0.60		
66	65.88±0.26		
90	44.13±0.16	30.78±0.12	33.41±0.13

Table 3: Relative detection efficiency vs illumination position

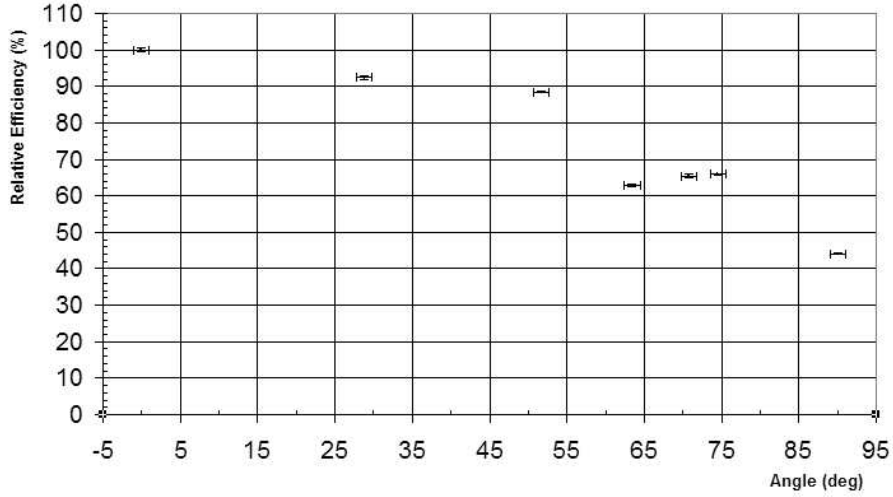


Figure 8: Relative detection efficiency as a function of the illumination position

2.2.2 Dependence on the incidence angle

The top of the photocathode (of PMT #1024) was illuminated under different incidence angles. The PMT was in the vertical position and the supply voltage was 1800V. The ratio of pulses measured for each incidence angle over the pulses at perpendicular incidence are shown as the pink dots in Figure 9. The blue dots are simulation results using the PMT model found in the Milagro Geant4 simulation code (g4sim). For incidence angles under about 55° the photons that pass through the glass and photocathode are incident on the internal structure of the PMT (dynodes or silvered part of the glass). The reflectivity of these surfaces is very high so most of the light after one or two reflections reaches the inside part of the photocathode for a second chance of being absorbed. Over 40deg the reflectivity of glass slowly starts to increase and as result the detection efficiency of the PMT decreases. The simulation was made with the PMT in air.

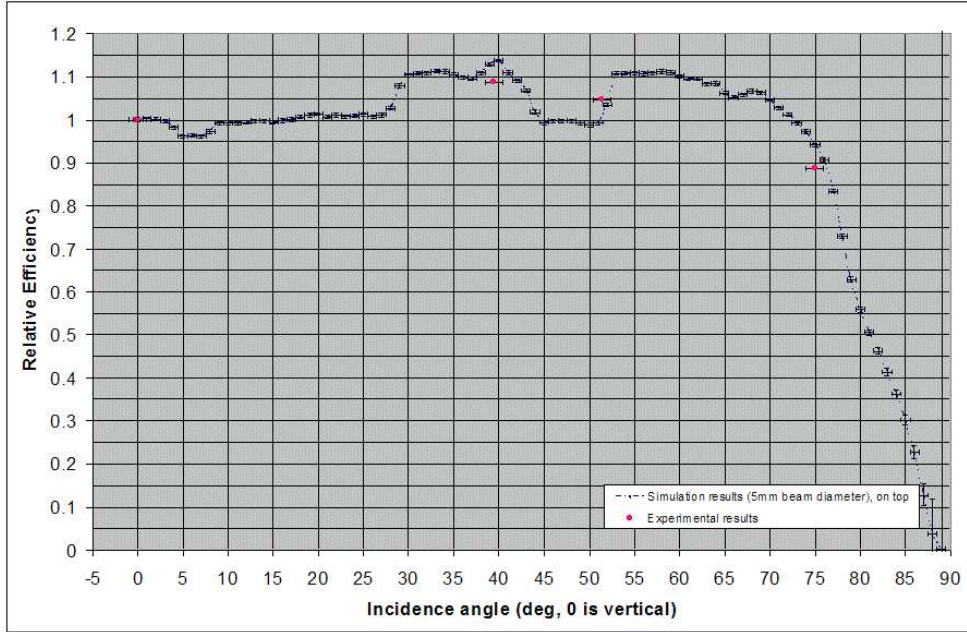


Figure 9: Relative detection efficiency as a function of the incidence angle

3 Discussion - Conclusion

The main reason for this series of tests was to better understand the behaviour of our PMTs and thus be able to simulate them more accurately. One of the biggest discrepancies between MC and data was the muon peak ². The muon peak for data would be around 100 pes while for the G4 MC it would be at least 180pes (depending on the simulated experimental conditions). There were thoughts that the actual PMT quantum efficiency was lower than the one used in the MC and a measurement of the detection efficiency was the initial motivation for this experiment.

After performing some tests on the photocathode uniformity, it was discovered that the PMT gain and the detection efficiency are strongly dependent on the position of the pe production on the photocathode. This could easily solve the muon peak problem without any further global corrections in the PMT efficiency. In this experimental work, there were some measurements made on the absolute detection efficiency of our PMTs. However, due to the bad stability of the available electronic instruments (the low voltage source was drifting) and to the low accuracy in the knowledge of the parameters involved in the analysis of the measurements, the final experimental results can't be trusted. For that reason, I chose to report them in the Appendix instead of in Chapter 2 along with the other tests. For the record, after correspondence of mine with a Hamamatsu representative, I was told that the detection efficiency of the Milagro PMTs³ shouldn't be considerably lower than the one reported in the spec sheets (a couple of percent at most in absolute values). Also I was told that we should expect a spread of at most 5-10% in the relative quantum efficiency from PMT to PMT.

Special code was written in Milinda to account for these effects. The pulse height spectra for different illumination positions and for the dark noise were saved in a data file (*milinda/config_milagro/pecurves.dat*). The new routine *milinda/code/GetPEAmp.c* initially rejects some of the detected pes from the MC depending on their detection position and later assigns random pulse heights to the rest of the pes using the saved pulse height spectra as the Probability Distribution Functions (PDF). The routine *milinda/code/AddNoise.c* adds cosmic and dark noise hits to the MC data. The pulse heights of the dark noise hits are produced using the dark noise pulse height spectrum as a PDF. The new code is used by default and can be found in Milinda v1.1 and newer.

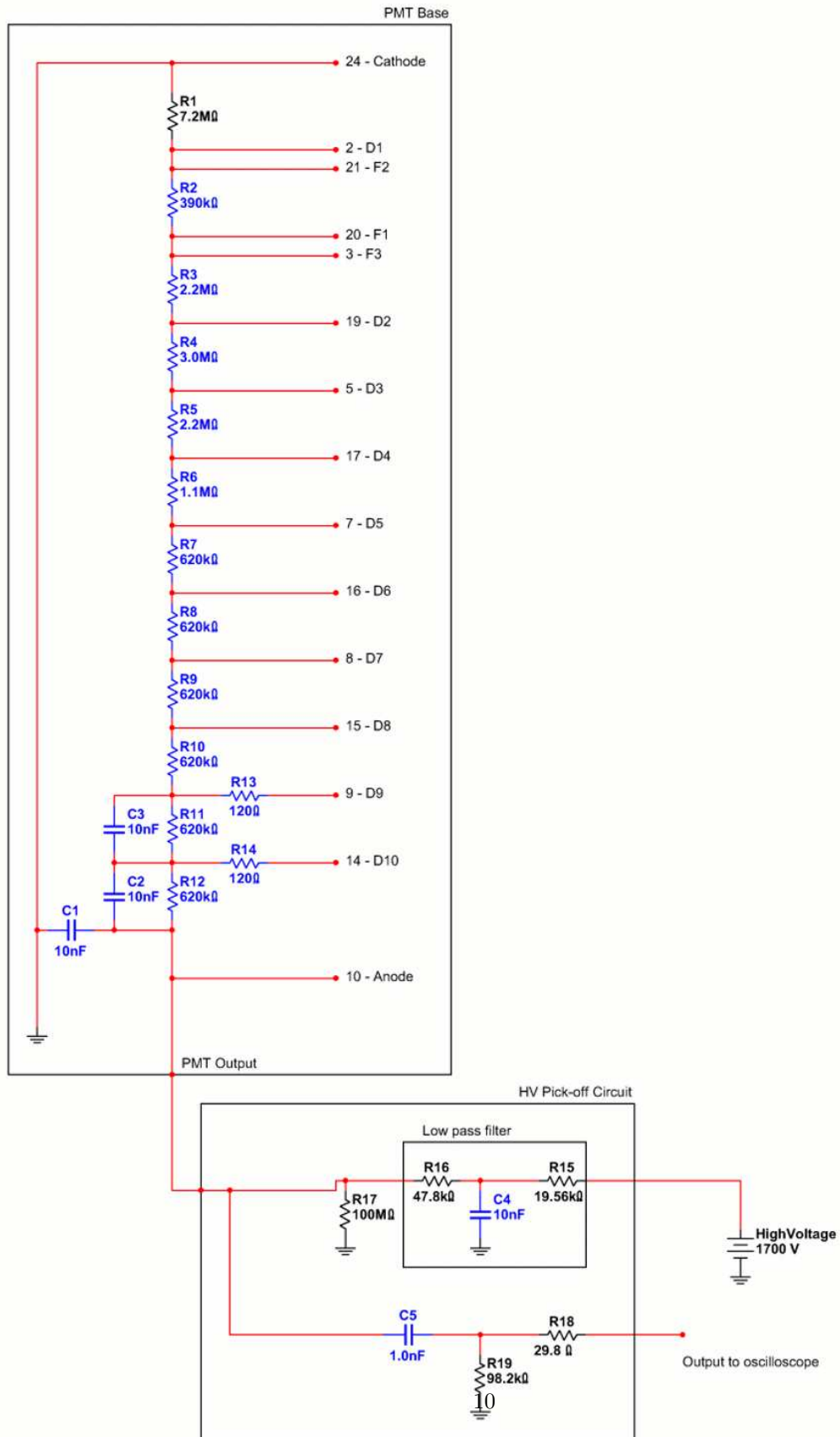
I would like to thank the NIST group (A. Migdall and S. Polyakov) for performing the calibration of the light source and B. Ellsworth, A. Smith and M. Coplan for helping me with all the problems I encountered in this experiment. I would also like to thank Nichia corp. for providing the LEDs.

²number of PEs in the muon layer caused by a muon

³R5912 PMTs of the age and previous usage similar to Milagro PMTs

4 Appendix

4.1 PMT Base and Signal pick-off circuit



4.2 Hamamatsu R5912 PMT Specifications

HAMAMATSU

PHOTOMULTIPLIER TUBE R5912

APPLICATIONS

- For High Energy Physics

GENERAL

Parameter		Description/Value	Unit
Spectral Response		300 to 650	nm
Wavelength of Maximum Response		420	nm
Photocathode	Material	Bialkali	—
	Effective Area	530 (Min. 450)	cm ² Typ.
Window Material		Borosilicate glass	—
Dynode	Structure	Box and Line	—
	Number of Stages	10	—
Direct Interelectrode	Anode to Last Dynode	3	pF
Capacitances (Approx.)	Anode to All Other Dynode	7	pF
Base		20-pin base JEDEC B20-102	—
Weight		Approx. 720	g
Suitable Socket		E678-20A (supplied)	—

CHARACTERISTICS (at 25°C)

Parameter		Min.	Typ.	Max.	Unit
Cathode Sensitivity	Luminous (2856K)	—	70	—	μA/lm
	Radiant at 420nm	—	72	—	mA/W
	Blue (CS 5-58 filter)	—	9.0	—	μA/lm-b
	Quantum Efficiency at 390nm	—	22	—	%
Anode Sensitivity ¹⁾	Luminous (2856K)	—	700	—	A/lm
	Radiant at 420nm	—	7.2 × 10 ⁵	—	A/W
Gain ¹⁾		—	1.0 × 10 ⁷	—	—
Supply Voltage for Gain of 10 ⁷		—	1500	1800	V
Anode Dark Current (after 30min. storage in darkness) ¹⁾		—	50	700	nA
Dark Count (after dark condition for 15 hours) ¹⁾		—	4	8	kcps
Time Response ¹⁾	Anode Pulse Rise Time	—	3.8	—	ns
	Electron Transit Time	—	55	—	ns
	Transit Time Spread (FWHM) ³⁾	—	2.4	—	ns
Pre Pulse ⁴⁾	4ns to 20ns before Main pulse	—	0.5	2	%
Late Pulse ³⁾	8ns to 60ns after Main pulse	—	1.5	3	%
After Pulse ³⁾	100ns to 16μns after Main pulse	—	2	10	%
Single Photoelectron	PHD (Peak to Valley Ratio)	—	2.5	—	—
Pulse Linearity ²⁾	at ±2% Deviation	—	60	—	mA
	at ±5% Deviation	—	80	—	mA
Magnetic characteristics (at 200mG/20μT)	Sensitivity Degradation	—	10	—	%

1) Measured with the condition shown in the Table 1. 2) Measured with the condition shown in the Table 2.

3) Measured with 0.25 photoelectrons detection threshold (at single photoelectron/ event).

4) Measured with 0.25 photoelectrons detection threshold (at 50 photoelectron/ event).

Subject to local technical requirements and regulations, availability of products included in this promotional material may vary. Please consult with our sales office. Information furnished by HAMAMATSU is believed to be reliable. However, no responsibility is assumed for possible inaccuracies or omissions. Specifications are subject to change without notice. No patent rights are granted to any of the circuits described herein. © 1998 Hamamatsu Photonics K.K.

PHOTOMULTIPLIER TUBE R5912

Table 1: VOLTAGE DISTRIBUTION RATIO AND SUPPLY VOLTAGE

Electrodes	K	Dy1	F2	F1	F3	Dy2	Dy3	Dy4	Dy5	Dy6	Dy7	Dy8	Dy9	Dy10	P
Ratio	11.3	0	0.6	0	3.4	5	3.33	1.67	1	1	1	1	1	1	1

Supply Voltage: 1500Vdc, K: Cathode, Dy: Dynode, P: Anode, F: Focus

Table 2: TAPERED VOLTAGE DISTRIBUTION RATIO FOR LINEARITY MEASUREMENT

Electrodes	K	Dy1	F2	F1	F3	Dy2	Dy3	Dy4	Dy5	Dy6	Dy7	Dy8	Dy9	Dy10	P
Ratio	11.3	0	0.6	0	3.4	5	3.33	1.67	1	1.2	1.5	2.2	3	2.4	
Capacitors in μF												0.01	0.01	0.01	

Supply Voltage: 1500Vdc, K: Cathode, Dy: Dynode, P: Anode, F: Focus

MAXIMUM RATINGS (Absolute Maximum Values)

Parameter	Value	Unit	
Supply Voltage	Between Anode and Cathode	1800	Vdc
	Between Anode and Last Dynode	300	V
Average Anode Current	0.1	mA	
Average Cathode Current	100	nA	
Ambient Temperature	-60 to +50	$^{\circ}\text{C}$	
Pressure	7	atm	

Figure 1: Typical Spectral Response

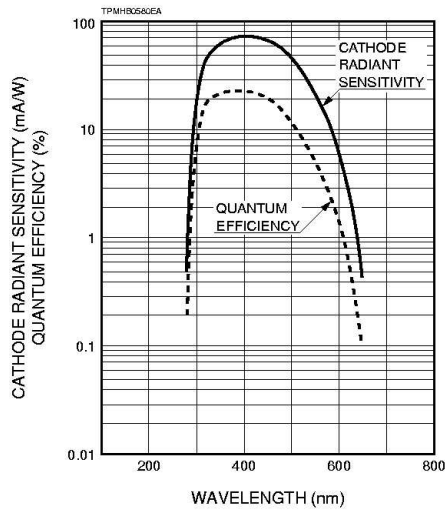


Figure 2: Typical Gain Characteristic

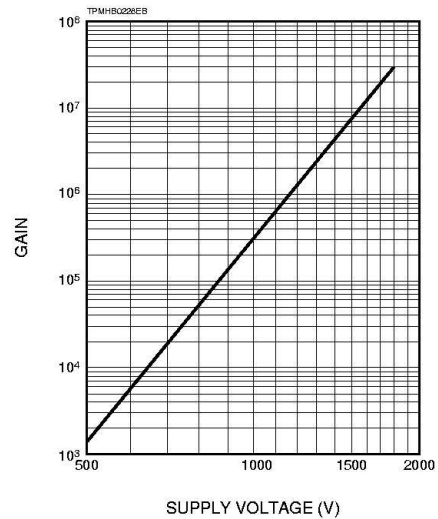


Figure 3: Pulse Height Distribution

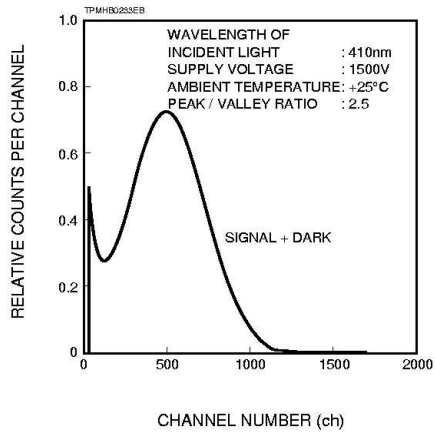


Figure 4: Transit Time Spread

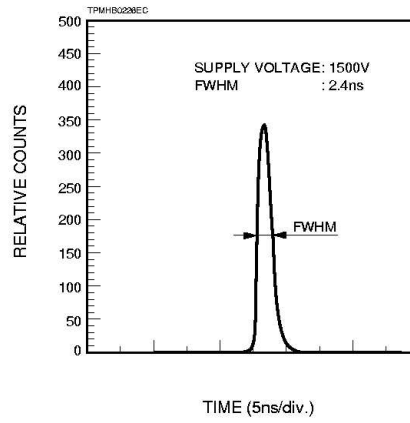
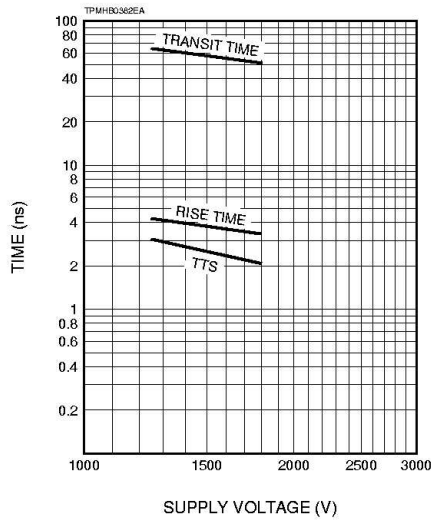
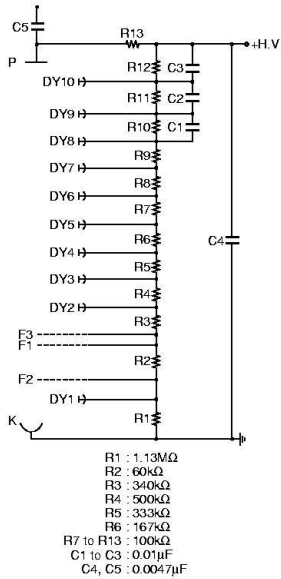
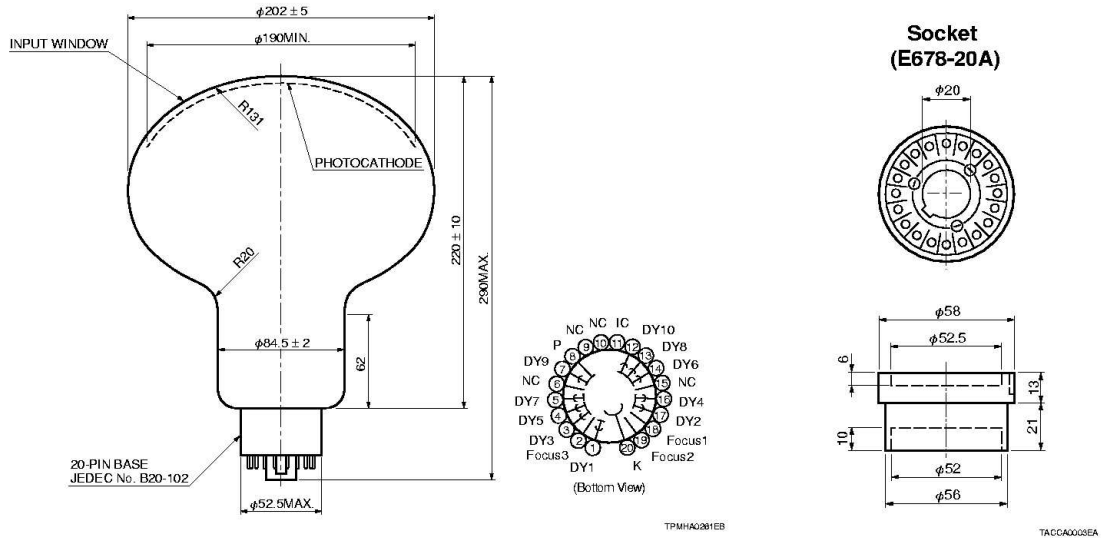


Figure 5: Typical Time Response



PHOTOMULTIPLIER TUBE R5912

Figure 6: Dimensional Outline and Voltage Divider (Unit: mm)



HAMAMATSU

HAMAMATSU PHOTONICS K.K., Electron Tube Center

314-5, Shimokanzo, Toyooka-village, Iwata-gun, Shizuoka-ken, 438-0193, Japan, Telephone: (81)539/62-5248, Fax: (81)539/62-2205

U.S.A.: Hamamatsu Corporation, 360 Foothill Road, P. O. Box 0810, Bridgewater, N.J. 08807-0910, U.S.A., Telephone: (1)908-231-0800, Fax: (1)908-231-1218

Germany: Hamamatsu Photonics Deutschland GmbH, Arzbergstr. 10, D-82211 Herrsching am Ammersee, Germany, Telephone: (49)8152-375-0, Fax: (49)8152-2858

France: Hamamatsu Photonics France S.A.R.L., 8, Rue du Saule Trépu, Parc du Moulin de Massy, 91882 Massy Cedex, France, Telephone: (33)1 68 53 71 00, Fax: (33)1 68 53 71 10

United Kingdom: Hamamatsu Photonics UK Limited, Lough Point, 2 Gladbeck Way, Windmill Hill, Enfield, Middlesex EN2 7JA, United Kingdom, Telephone: (44)181-367-3580, Fax: (44)181-367-8384

North Europe: Hamamatsu Photonics Norden AB, Färdgatan 7, S-184-40 Kista Sweden, Telephone: (46)8-703-29-50, Fax: (46)8-750-58-95

Italy: Hamamatsu Photonics Italia S.R.L., Strada della Moia, 1/E, 20020 Arese, (Milano), Italy, Telephone: (39)02-835 81 733, Fax: (39)02-835 81 741

TPMH1235E01
 SEPT. 1998 IP

4.3 Absolute measurement of the detection efficiency of the PMT

Finally, an absolute measurement of the PMT detection efficiency was made for two different wavelength ranges. The Nichia Blue NSPB518S and Green NSPG518S LEDs were used. Initially, the spectrum of the LEDs was taken using a spectrometer at NIST. The measurement results, corrected for the wavelength-dependent efficiency of the spectrometer, are shown in Figure 10. These spectra were fitted and two spectral weight functions were produced. By folding these functions with the wavelength dependent properties⁴, the effective value of these properties for each LED could be found.

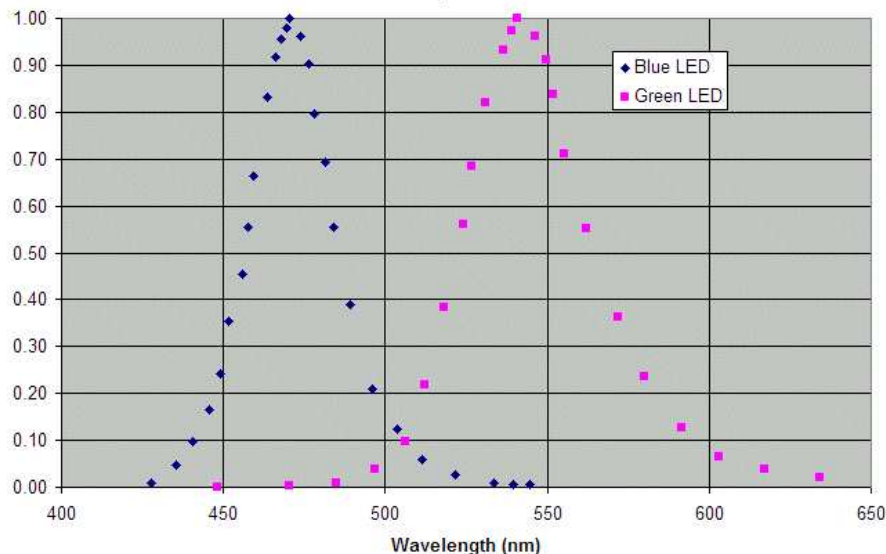


Figure 10: Spectra of the LEDs used in the light source

Afterwards, the light source was calibrated using a calibrated photodiode at NIST⁵. Because a photodiode likes to detect higher light levels than a PMT, the light source was calibrated without the ND2 filter. The effective area of the photodiode was a 5.8mm square and the beam had a circular aperture of ~ 5 mm in diameter, so no light was spilling in the non-effective area of the photodiode. The photodiode’s voltage, which was proportional to the light intensity detected by it, was recorded for each supply voltage of the LED (Figure 11). The LED was operated at the voltage levels where it would produce the low light levels suitable for use with the PMT. Using the photodiode’s responsivity data, its voltage could be converted to detected light intensity. The photodiode voltage was converted to a current, using a resistance value which was equal to the gain in Ohms ($10^9\Omega$). Afterwards, using the photodiode’s responsivity (Figure 12), this current was converted to the light power detected. Using the spectra of the LEDs, an average photon energy was calculated for each LED and using this number the light intensity detected by the photodiode was derived.

The neutral density filter absorptivity is almost flat with wavelength. The actual absorption factor for the two spectra was calculated by folding the filter absorption spectrum ((Figure14) with the LED spectra. The results were very close to 100. The dark and signal counts from the PMT were measured for a period of 10sec. The scaler had a dead time of about 20nsec. So the dead time of the system was the number of triggers times 20nsec. The signal detection rate was calculated by dividing the signal minus background counts, corrected for the reduced counting efficiency⁶, with the live time. By multiplying this rate with the calculated filter absorption factor, the light intensity that would be detected from a light source without a filter was found. This last rate is the appropriate number to be compared with the calibration measurements performed at NIST. The ratio of the the light intensity detected from a source without a filter (PMT

⁴Photodiode responsivity, filter absorption factor, PMT quantum efficiency

⁵by Alan Migdall and Sergey Polyakov

⁶see discussion in Chapter ?? on page ??

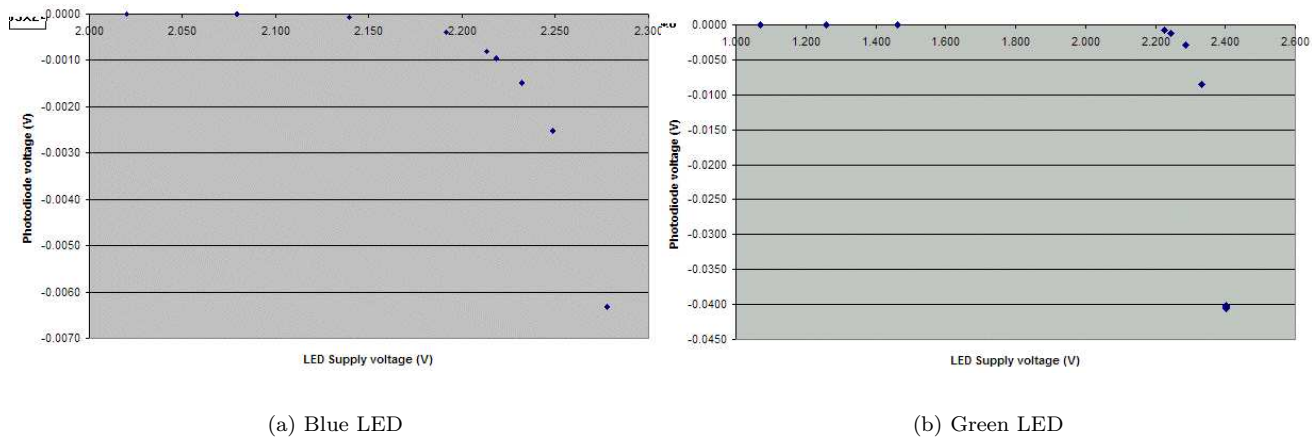


Figure 11: Photodiode voltage vs LED supply voltage

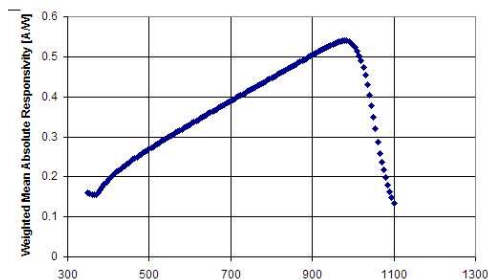
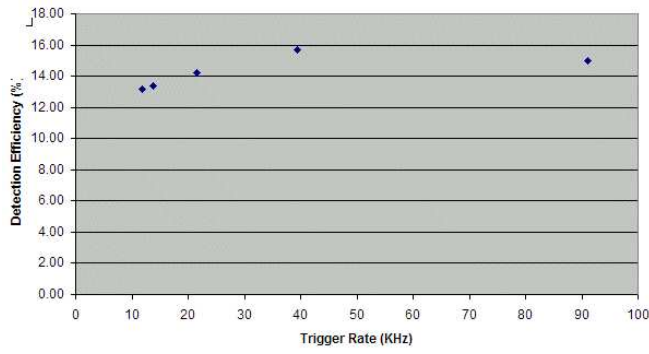


Figure 12: Photodiode spectral response

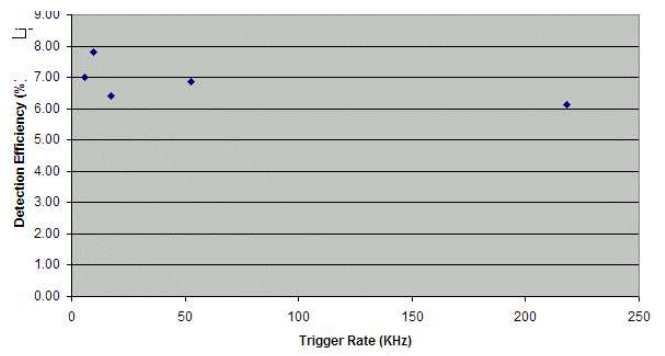
measurements) over the light intensity produced (NIST calibration) is equal to the PMT detection efficiency. The measurements were repeated for the various light levels calibrated at NIST. The detection efficiency measured versus different counting rates can be found in Figure 13 . The final result along the expected PMT detection efficiency from the PMT specs can be found in Table 4.

LED	QE from the specifications (%)	Measured detection efficiency (%)
Blue	16.35	15.69±0.53
Green	5.84	6.61±0.31

Table 4: Measured detection efficiency



(a) Blue LED



(b) Green LED

Figure 13: Detection efficiency measured for various trigger rates

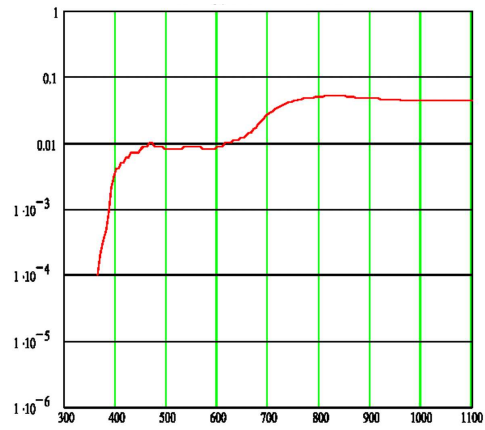


Figure 14: Thorlabs ND2 Typical Transmission Plot